Eurasian Chem.-Technol. J. 27 (2025) 315–321

The journal of the Institute of Combustion Problems https://ect-journal.kz

https://doi.org/10.18321/ectj1678

Aromatase (CYP19A1) Inhibitory Activity of Coltsfoot (*Tussilago farfara* L.) Phytochemicals: *In Vitro* and *in Silico* Evaluation

Izaz Ahmad[1,2], Muhammad Atif[3], Gulmaira Aldibekova[4], Didara Balpanova[4], Humaira Zafar[5], Maria Sadia[2], Mushtaq Ahmad[6], Atia-tul-Wahab[5], Bates Kudaibergenova[1]*, Muhammad Iqbal Choudhary[1,3,5]

[1]Al-Farabi Kazakh National University, Almaty 050040, Kazakhstan
[2]Department of Chemistry, University of Malakand, Chakdara, Lower Dir 18800, Pakistan
[3]H.E.J. Research Institute of Chemistry, International Center for Chemical and Biological Sciences, University of Karachi, Karachi 75270, Pakistan
[4]School of Pharmacy, S.D. Asfendiyarov Kazakh National Medical University, Almaty 050000, Kazakhstan
[5]Dr. Panjwani Center for Molecular Medicine and Drug Research, International Center for Chemical and Biological Sciences, University of Karachi, Karachi 75270, Pakistan
[6]Department of Higher Education Khyber Pakhtunkhwa, Govt, College Wari Upper Dir 18200, Pakistan

Article info

Received:
12 May 2025

Received in revised form:
6 July 2025

Accepted:
30 August 2025

Keywords:
Anticancer
Aromatase
Natural products
Molecular docking
Exemestane

Abstract

Estrogen plays a critical role in the development and progression of hormone-sensitive breast cancer. Aromatase (CYP19A1), the key enzyme catalyzing the final step in estrogen biosynthesis, has emerged as a promising therapeutic target. Although third-generation synthetic aromatase inhibitors (AIs) are effective, their use is limited by serious side effects, highlighting the need for safer natural alternatives. In this study, we evaluated three major flavonoids from *Tussilago farfara* L., quercetin-3-rutinoside (**1**), quercetin-3-*O*-β-D-glucoside (**2**), and kaempferol-3-*O*-glucoside (**3**) for aromatase inhibitory potential. *In vitro* assays showed that compound **3** was the most potent (IC_{50} = 3.46 μM), followed by compound **2** (3.79 μM) and compound **1** (3.81 μM), with activities comparable to potent dietary flavonoids and stronger than some reported natural analogues. Molecular docking supported these findings, showing favourable docking scores (-6.73 to -4.19) and binding energies (-60.3 to -43.7 kcal mol^{-1}), comparable to those of the standard inhibitor exemestane (IC_{50} = 0.20 μM; -68.3 kcal mol^{-1}). However, the computational predictions did not fully replicate the experimental ranking, reflecting the limitations of docking methods. Overall, these results highlight the significance and therapeutic potential of *T. farfara* flavonoids as natural aromatase inhibitors.

1. Introduction

Cancer remains a primary cause of death worldwide, with rising rates in both developed and developing countries. In 2020, roughly 19.3 million new cancer cases, and 10 million cancer-related deaths were reported worldwide, with breast cancer accounting for 11.7% of all cases [1]. In Egypt, breast cancer accounts for around 38.85% of all female cancer cases [2]. Epidemiological research confirms that extended estrogen exposure considerably raises the risk of developing breast cancer [3]. Furthermore, androgens such as testosterone, which are converted to estrogens by the enzyme aromatase, have been related to an increased risk of breast cancer, regardless of other recognized risk factors [4, 5].

Aromatase (CYP19A1) is a key enzyme that converts male hormones (androstenedione, testosterone) into female hormones (estrone, estradiol). This is the final step stage in steroid production [6]. Hence, aromatase is an important therapeutic target for estrogen suppression [7, 8]. Aromatase activity in the tumor microenvironment is especially important in postmenopausal women because breast cancers produce local estrogen, which drives cancer growth [9, 10]. As a result, successful therapy requires

---

*Corresponding author.
E-mail address: bateskudaibergenova@yahoo.com

targeting both peripheral, and elevated levels of intratumoral aromatase [11]. Early aromatase inhibitors (AIs), such as aminoglutethimide, successfully lowered estrogen levels but lacked selectivity, resulting in undesired inhibition of other steroidogenic pathways and side effects such as cortisol, and aldosterone suppression [5, 12]. Second-generation AIs such as formestane (steroidal), and fadrozole (nonsteroidal) had improved potency and safety profiles, but their selectivity and clinical efficacy remained inferior to tamoxifen [13, 14]. Third-generation AIs, including anastrozole, letrozole (nonsteroidal), and exemestane (steroidal) provided better selectivity and clinical results; however, vorozole were withdrawn due to minimal benefit [15]. Despite these developments, the need for safer, more effective, and less expensive alternatives remains [16].

Natural products have long been important resources in anticancer drug discovery, with several studies continuing to investigate their therapeutic potential [17]. *Tussilago farfara* L. (coltsfoot), a perennial herb traditionally used to treat respiratory disorders, includes about 150 phytochemicals such as flavonoids, sesquiterpenes, triterpenoids, phenolics, and alkaloids [18, 19]. Various flavonoids, such as chrysin [20], apigenin [21], and kaempferol [22], which are found naturally, have been reported to inhibit aromatase *in vitro*. Nevertheless, the aromatase-inhibitory properties of the dominant flavonoids of *Tussilago farfara* L., quercetin-3-rutinoside, quercetin-3-*O*-D-glucoside, and kaempferol-3-*O*-D-glucoside, have not been explored.

Since the plants are rich in phytochemistry and have an extensive history of therapeutic application, we considered them as potential natural aromatase inhibitors. In particular, this paper looks at them in vitro inhibitory activity and in silico interactions with aromatase and also conducts molecular docking, which shows that they have binding energies similar (although slightly lower) to the standard aromatase inhibitor exemestane and thus are a promising scaffolds to construct safer aromatase inhibitors.

2. Experimental

2.1. Plant material

The aerial parts of the *Tussilago farfara* (10 kg) (Fig. 1) were collected in April 2023 from the Ile-Ala-Tau State National Natural Park near Almaty, Kazakhstan (76°30′12″–77°50′27″ E, 42°48′30″–43°19′35″ N) at an altitude of approximately 800 meters above sea level. The species was authenticated and validated by Professor G.T. Sitpayeva of the Botany Institute and Phytointroduction, Almaty, Kazakhstan (Accession number: 3318).

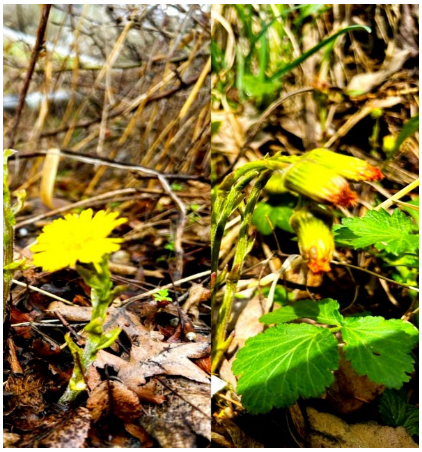

Fig. 1. *Tussilago farfara* L., flower buds and bloomed flowers.

2.2. Isolation and purification

Isolation and purification of the quercetin-3-rutinoside **(1)**, quercetin-3-*O*-β-D-glucoside **(2)**, and kaempferol 3-*O*-glucoside **(3)** have been published [23]. Here we are focusing in the aromatase potential of the purified compounds *in vitro*, and *in silico*.

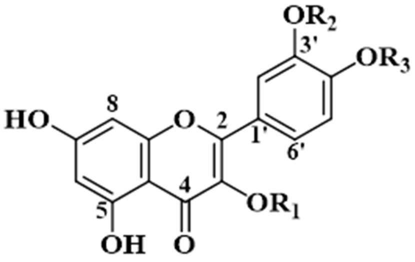

	R_1	R_2	R_3
1:	ORut	OH	OH
2:	OGlu	OH	OH
3:	OGlu	H	OH

Fig. 2. Chemical structures of active compounds against aromatase.

2.3. In vitro studies

The *in vitro* human placental aromatase inhibition experiment was carried out utilizing a previously known technique. The experiment used a 96-well black fluorescent plate with a final reaction volume of 200 µL. The test compounds were dissolved in DMSO, and the substrate, 7-methoxy-4-(trifluoromethyl)coumarin (MFC) was prepared in acetonitrile. The enzyme solution contained 2 mg/mL of human placental microsomes suspended in 0.1 M potassium phosphate buffer (pH 7.4) and was mixed with MFC to reach a final substrate concentration of 25 µM. To start the assay, 5 µL of each test compound at different doses was added to 95 µL of enzyme-substrate combination in each well. The plate was pre-incubated at 37 °C for 5 minutes. To start the reaction, 100 µL of NADPH (1 mM) was added to each well, bringing the total volume to 200 µL. After a 20-minute incubation at 37 °C, the reaction was stopped by adding 75 µL of acetonitrile (0.1 M of Tris base). Fluorescence measurements were taken with a Kanlt-lux plate reader at an excitation wavelength of 400 nm and emission at 540 nm to quantify metabolite production and aromatase inhibition [24]. Background fluorescence was measured by adding the stop solution to wells containing the enzyme-substrate mixture before adding NADPH, which prevented the enzymatic process. Under the assay conditions, metabolite production was found to be linear in terms of incubation duration and protein concentration. We obtained the IC_{50} values, which represent the concentration of each test chemical necessary to inhibit 50% of enzyme activity, by fitting the fluorescence data to a dose-response curve using GraphPad Prism 5 [25].

$$(IC_{50}) = \frac{50 - A}{B - A} \times (D - C) + C$$

where, A is less than 50% of inhibition and B is higher than 50% of inhibition. C is the concentration of low inhibition A and D is the concentration of high inhibition B.

2.4. In silico studies

2.4.1. Ligand Preparation

Ligands were prepared using the LigPrep program, which optimized their structures by changing torsional angles, assigning appropriate protonation states, producing relevant stereoisomers, and estimating the most likely ionization states at pH 7.0 ± 2.0 [24].

2.4.2. Molecular Docking Studies

Molecular docking investigations were carried out using Schrödinger Suite 2023-1's Glide 6.9 module. The docking was done with the crystal structure obtained from the Protein Data Bank (PDB ID: 4KQ8). To characterize the active site, a receptor grid (10 × 10 × 10 Å) was generated, centered on the co-crystallized ligand, 4-androstene-3,17-dione. Ligands were docked in Glide XP (extra precision) mode, and the top poses were selected based on the lowest (most negative) docking scores, which reflect stronger binding affinity. The Glide scoring function evaluates hydrogen bonding, hydrophobic contacts, steric and electrostatic interactions, and desolvation effects to identify the most stable ligand–protein conformations [26].

2.4.3. MM-GBSA tool for Binding Energy Estimation

Molecular docking is a computer technique that predicts the most favorable orientation of a ligand when it binds to a protein, resulting in a stable compound. The Molecular Mechanics-Generalized Born Surface Area (MM-GBSA) method estimates the binding free energy between a ligand and a protein by combining molecular mechanics energies with implicit solvent and surface area term represents non-polar solvation effects, providing an overall assessment of binding affinity [27]. The Prime MM-GBSA module from Schrödinger Suite 2023-1 was used to assess binding affinity and optimize docked postures. This utility reranked the ligand conformations produced by Glide XP docking and estimated their respective binding free energies. A lower binding energy value (kcal mol^{-1}) indicates a higher expected binding affinity between the ligand and protein [28, 29].

3. Results and Discussion

3.1. Structure elucidation of compounds (1-3)

The structural elucidation of quercetin-3-rutinoside **(1)**, quercetin-3-*O*-β-D-glucoside **(2)**, and kaempferol 3-*O*-glucoside **(3)** has been reported previously [23].

Here the *in vitro* human placental aromatase experiment was carried out. Compounds **(1-3)** were found to be active against the aromatase, which is directly involved in human breast cancer. These compounds showed IC_{50} values in the range of 3.46 ± 0.002 µM to 3.81 ± 0.001 µM. For instance, compound **1** showed an IC_{50} value of 3.81 ± 0.002 µM. Similarly, compound **2** indicated 3.79 ± 0.001 µM, while compound **3** showed 3.46 ± 0.002 µM, which showed notable inhibition of the human placental aromatase activity as compared to the standard anticancer drug exemestane (IC_{50} = 0.204 ± 0.051 µM). Yet the tested flavonoids remained active within the low-micromolar range, indicating meaningful biological potential.

Our findings (IC_{50} = 3.46–3.81 µM) are comparable to the potent flavonoid chrysin (IC_{50} ~ 4.6 µM) [20] and stronger inhibitory potential than kaempferol (Ki ~ 27 µM) (although it should be noted that IC_{50} and Ki values are not directly interchangeable) [22]. To the best our knowledge, this is the first report of these *T. farfara* flavonoids as aromatase inhibitors. Moreover, our molecular docking results showed binding energies of -60.3, -51.8, and -43.7 kcal mol^{-1} and docking scores -6.73 to -4.19, which are comparable, though somewhat weaker, to the standard aromatase inhibitor exemestane (binding energy -68.3 kcal mol^{-1}), thereby supporting the biochemical findings (Fig. 3 and Table 1).

Within our series, compound **3** (kaempferol-3-*O*-glucoside, IC_{50} = 3.46 µM) was the most potent. A likely explanation is the influence of glycosylation pattern and steric bulk: larger or more complex sugar moieties (e.g., the rutinoside in compound **1**) increase polarity and steric hindrance, which can reduce access and optimal fitting into the aromatase active site compared with smaller glucosides. This general effect of *O*-glycosylation reducing immediate enzyme-inhibitory potency (while improving solubility and stability) has been noted in comparative studies of flavonoid glycosides versus aglycones [30].

Despite the fact that, the MM-GBSA rescoring and docking showed that compound **1** would bind best (docking score -6.73; MM-GBSA = -60.33 kcal mol^{-1}), it was experimentally found that compound **3** is the strongest (IC_{50} of 3.46 µM). Such deviation is no surprise: docking and rescoring algorithms are estimating largely enthalpic, static binding, and are machine dependent, scoring functions and receptor/ligand preparation, and experimental potency is also determined by solubility, permeability, dynamics and assay conditions. Thereby, docking/MM-GBSA is to be taken qualitatively in order to justify binding modes in our dataset but not as predictors of the IC_{50} values [31].

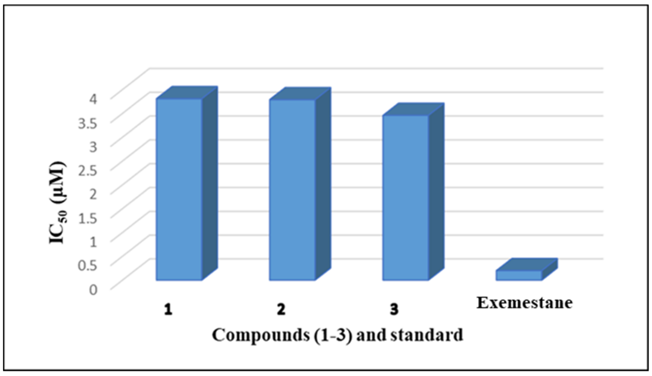

Fig. 3. Comparison of IC_{50} values of compounds **1-3** and exemestane for aromatase inhibition.

Table 1. The IC_{50} values, docking score, and MM-GBSA binding energies of compounds **1-3** and standard exemestane.

No	Compounds	IC_{50} ± µM	Docking Score	MM-GBSA (Kcal/mol)
1	1	3.81 ± 0.002	-6.734	-60.33
2	2	3.79 ± 0.001	-4.291	-44.68
3	3	3.46 ± 0.002	-4.198	-43.70
5	Exemestane^a	0.204± 0.051	-6.01	-68.31

^{a}Positive control

Protein-ligand docking has several limitations. Most docking methods use a rigid protein approximation where the ligand is flexible but the protein conformation is restricted [32]. Docking poses and scores can also depend strongly on the ligand input structure, so small conformational differences may lead to large variations in the results [33]. Importantly, the scoring functions used do not always provide a reliable prediction of binding affinity [34], and the best energy score is not necessarily a reliable criterion for compound activity [35]. Docking scores from different programs also cannot be directly compared because they depend on the specific force fields and protocols applied [36]. In addition, handling of water molecules in the binding site can affect the accuracy of predicted interactions [31], and the ability of docking to separate active compounds from decoys is strongly influenced by the protein structure used and the similarity to co-crystallized ligands [37].

Consequently, although a direct relationship between docking scores, binding energies, and experimental inhibitory activity might be expected theoretically, no consistent linear correlation is typically observed. This discrepancy reflects the combined effects of biological variability, target-specific responses, and differences in experimental conditions [38].

Compound **1** showed the highest docking score of -6.734 against the aromatase enzyme, which is actively involved in breast cancer (Fig. 5). Compound **1** suggest a good network of interactions with the active pocket of the receptor protein. For instance, the OH group at C-8 of ring 1 showed an H-bond. Similarly, the OH group at C-3' of ring 3 formed the H-bond with the amino acids ILE132 and ARG 115. The OH group at C-4' showed an H bond with TRP 141. In ring 5, the hydroxyl groups located at C-2''' and C-4''' established the aromatic H-bond and H-bond with the amino acids PHE 430 and PRO 429 consecutively (Fig. 4). The protein-ligand complex showed a high negative binding energy of -60.33 kcal mol^{-1}, which indicated the stability of compound **1** with the receptor protein aromatase (Fig. 6).

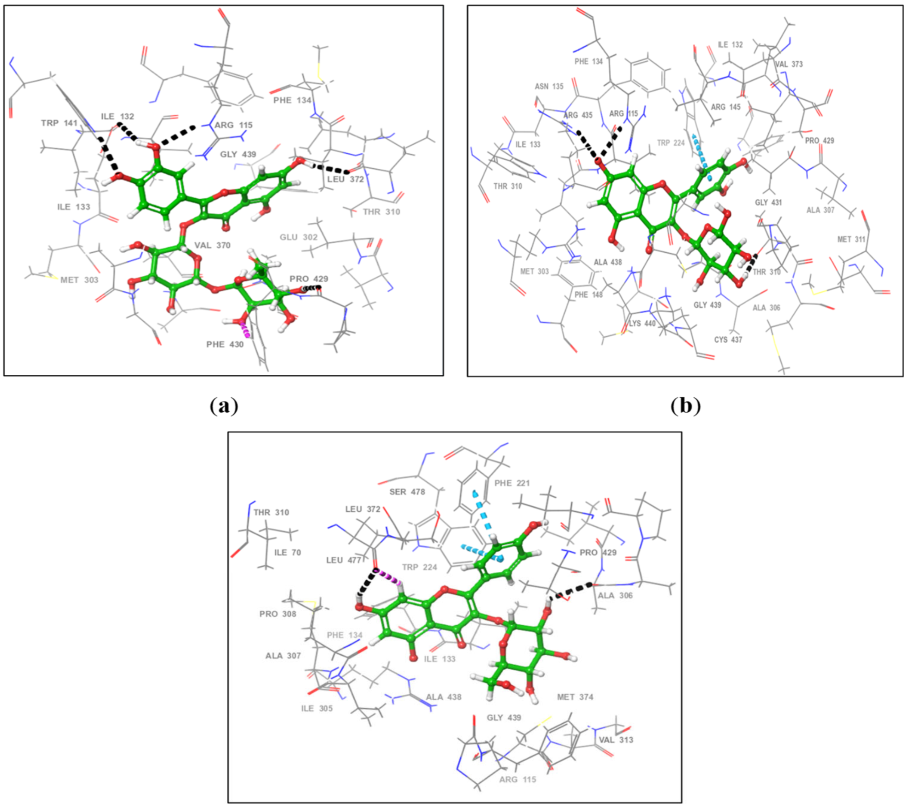

(a) (b)

(c)

Fig. 4. 3D-docked pose of compound 1 (a), 2 (b), and 3 (c) with the active domains of aromatase. The black, pink, and blue dotted lines showed the hydrogen, aromatic H, and π-π stacking bonding interactions respectively.

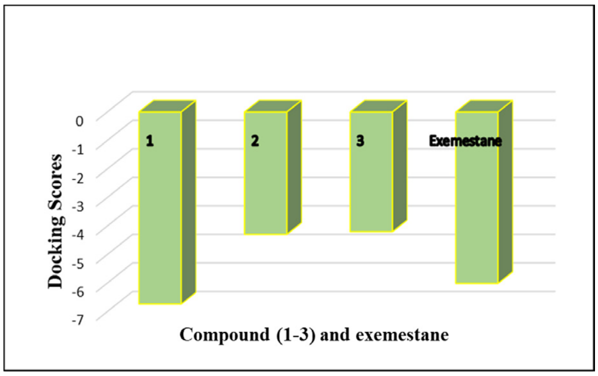

Fig. 5. Docking scores of compounds 1-3 and exemestane against aromatase (CYP19A1).

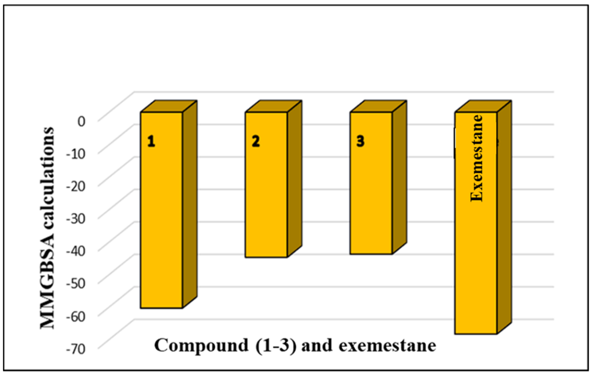

Fig. 6. Binding energy affinity of compounds 1-3 and exemestane with aromatase.

Compound **2** showed a docking score of -4.291 (Fig. 5). It showed best network of interactions with the receptor protein. For instance, the OH group at C-8 of ring 1 showed two H-bonds with the amino acids ARG 435 and ARG 115 consecutively. Ring 3 of the compound **2** formed the π-π stacking interactions with TRP 224. The hydroxyl group at C-3" of ring 4 showed the H-bond with the THR 310 located at the active site of the receptor protein (Fig. 4). To estimate the stability of the protein-ligand complex, the MM-GBSA tool showed a binding energy of -44.68 kcal mol^{-1}, which indicated the stability of compound **2** with the receptor protein (Fig. 6).

Compound **3** showed a docking score of -4.198 (Fig. 5). This demonstrates three different types of noncovalent interactions. For instance, the OH group attached at C-8 of ring 1 formed the H-bond, while the proton at C-9 exhibited the aromatic H-bond with the amino acid LEU 477. Similarly, ring 3 formed two π-π stacking interactions with TRP 224 and PHE 221 consecutively. The hydroxyl group attached at C-2" of ring 4 showed the H-bond with the amino acid ALA 306 (Fig. 4). The protein-ligand complex showed the binding energy -43.70 kcal/mol and exhibited the stability of compound **3** at the active site of aromatase (Fig. 6).

4. Conclusion

This study emphasizes the potential of some phytochemicals from *Tussilago farfara* L. as natural aromatase (CYP19A1) inhibitors. *In vitro*, the flavonoids quercetin-3-rutinoside **(1)**, quercetin-3-O-β-D-glucoside **(2)**, and kaempferol-3-*O*-glucoside **(3)** showed notable aromatase inhibitory activity in the low micromolar range. Among these, compound **3** (kaempferol-3-*O*-glucoside) was the most potent *in vitro*. Molecular docking and binding energy analyses supported these findings by revealing favourable ligand-enzyme interactions, although computational predictions did not perfectly reproduce experimental potency. The docking profiles showed similar binding patterns to those of the reference inhibitor exemestane, indicating a plausible binding mechanism rather than meaningful inhibition. Overall, these findings suggest that *T. farfara* derived flavonoids represent promising leads for the development of safer, plant-based aromatase inhibitors for estrogen-dependent breast cancer. Further *in vivo* studies and clinical validation will be essential to establish their efficacy, pharmacokinetic properties, and safety profiles.

Acknowledgment

I.A. is thankful to Al-Farabi Kazakh National University (Almaty, Kazakhstan) for financial support, and the authors also appreciate the ICCBS for logistical support.

References

[1]. H. Sung, J. Ferlay, R. Siegel, et al., Global cancer statistics 2020: GLOBOCAN estimates of incidence and mortality worldwide for 36 cancers in 185 countries, *CA Cancer J Clin.* 71 3 (2021) 209–249. DOI: 10.3322/caac.21660

[2]. S.K. Mohamed, Awareness and knowledge toward breast cancer and breast self-examination: A cross-sectional descriptive study among undergraduate female students at Cairo University, Egypt, *Malays. J. Nurs.* 12 (2021) 111–119. DOI: 10.31674/mjn.2021.v12i03.013

[3]. J.D. Yager, N.E. Davidson, Estrogen carcinogenesis in breast cancer, *N. Engl. J. Med.* 354 (2006) 270–282. DOI: 10.1056/NEJMra050776

[4]. W.R. Miller, A.P.M. Forrest, Oestradiol synthesis by a human breast carcinoma, *Lancet* 304 (1974) 866–868. DOI: 10.1016/S0140-6736(74)91202-1

[5]. A.S. Bhatnagar, A.M.H. Brodie, B.J. Long, et al., Intracellular aromatase and its relevance to the pharmacological efficacy of aromatase inhibitors, *J. Steroid Biochem. Mol. Biol.* 76 (2001) 199–202. DOI: 10.1016/S0960-0760(01)00050-4

[6]. D.R.P. Guay, Aromatase inhibitors in breast cancer, *Am J Geriatr Pharmacother.* 2 (2004) 149–150. DOI: 10.1016/S1543-5946(04)80040-0

[7]. M. Correia, P. Hollenberg, Inhibition of Cytochrome P450 Enzymes. In: Ortiz de Montellano, P. (eds) Cytochrome P450. Springer, Cham. (2015) 177–259. DOI: 10.1007/978-3-319-12108-6_5

[8]. F. Rasha, M. Sharma, K. Pruitt, Mechanisms of endocrine therapy resistance in breast cancer, *Mol. Cell. Endocrinol.* 532 (2021) 111322. DOI: 10.1016/j.mce.2021.111322

[9]. K. Luo, J. Liu, Y. Wang, et al., Associations between organophosphate esters and sex hormones among 6–19-year old children and adolescents in NHANES 2013–2014, *Environ. Int.* 136 (2020) 105461. DOI: 10.1016/j.envint.2020.105461

[10]. L. Guo, D. Kong, J. Liu, et al., Breast cancer heterogeneity and its implication in personalized precision therapy, *Exp. Hematol Oncol.* 12 (2023) 3. DOI: 10.1186/s40164-022-00363-1

[11]. A.S. Bhatnagar, The discovery and mechanism of action of letrozole, *Breast Cancer Res. Treat.* 105 (Suppl 1) (2007) 7–17. DOI: 10.1007/s10549-007-9696-3

[12]. D.J.L. Ghosh, C. Egbuta, Recent progress in the discovery of next generation inhibitors of aromatase from the structure–function perspective, *J. Med. Chem.* 59 (2016) 5131–5148. DOI: 10.1021/acs.jmedchem.5b01281

[13]. R.J. Santen, L.M. Demers, J. Lynch, et al., Specificity of low dose fadrozole hydrochloride (CGS 16949A) as an aromatase inhibitor, *J. Clin. Endocrinol. Metab.* 73 (1991) 99–106. DOI: 10.1210/jcem-73-1-99

[14]. C.I. Falkson, H.C. Falkson, A randomised study of CGS 16949A (fadrozole) versus tamoxifen in previously untreated postmenopausal patients with metastatic breast cancer, *Ann. Oncol.* 7 (1996) 465–469. DOI: 10.1093/oxfordjournals.annonc.a010634

[15]. A.U. Buzdar, Pharmacology and pharmacokinetics of the newer generation aromatase inhibitors. *Clin Cancer Res.* 9 (2003) 468s-472s. https://aacrjournals.org/clincancerres/article/9/1/468s/289362/Pharmacology-and-Pharmacokinetics-of-the-Newer

[16]. J.C. Bailar, H.L. Gornik, Cancer undefeated, *N. Engl. J. Med.* 336 (1997) 1569–1574. DOI: 10.1056/NEJM199705293362206

[17]. A.L. Harvey, R.E. Ebel, R.J. Quinn, The re-emergence of natural products for drug discovery in the genomics era, *Nat. Rev. Drug Discov.* 14 (2015) 111–129. DOI: 10.1038/nrd4510

[18]. C. Liu, H. Wu, L. Wang, et al., Farfarae Flos: A review of botany, traditional uses, phytochemistry, pharmacology, and toxicology, *J. Ethnopharmacol.* 260 (2020) 113038. DOI: 10.1016/j.jep.2020.113038

[19]. S. Chen, L. Dong, H. Quan, et al., A review of the ethnobotanical value, phytochemistry, pharmacology, toxicity and quality control of Tussilago farfara L. (coltsfoot), *J. Ethnopharmacol.* 267 (2021) 113478. DOI: 10.1016/j.jep.2020.113478

[20]. D.R. Campbell, M.S. Kurzer, Flavonoid inhibition of aromatase enzyme activity in human preadipocytes, *J. Steroid Biochem. Mol. Biol.* 46 (1993) 381–388. DOI: 10.1016/0960-0760(93)90228-o

[21]. C. Wang, T. Mäkelä, T. Hase, H. Adlercreutz, M.S. Kurzer, Lignans and flavonoids inhibit aromatase enzyme in human preadipocytes, *J. Steroid Biochem. Mol. Biol.* 50 (1994) 205–212. DOI: 10.1016/0960-0760(94)90030-2

[22]. H.J. Jeong, Y.G. Shin, I.H. Kim, J.M. Pezzuto, Inhibition of aromatase activity by flavonoids, *Arch. Pharm. Res.* 22 (1999) 309–312. DOI: 10.1007/BF02976369

[23]. I. Ahmad, B. Kudaibergenova, M. Ahmad, et al., Coltsfoot (Tussilago farfara L.; Asteraceae): modern methods of extraction, phytochemistry, nanoparticles synthesis, ethnopharmacology, and biological activities. *Nat Prod Res*. (2025). DOI: 10.1080/14786419.2025.2548616

[24]. H. Li, Y. Zhao, L. Chen, et al., Triclocarban and triclosan inhibit human aromatase via different mechanisms, *Biomed Res. Int.* (2017) 8284097. DOI: 10.1155/2017/8284097

[25]. H. Zafar, R. Anis, S. Hafeez, et al., Identification of Non-steroidal Aromatase Inhibitors via In silico and In vitro Studies, *Med. Chem.* 19 (2023) 986–1001. DOI: 10.2174/1573406419666230330082426

[26]. S.G. Madhavi Sastry, M. Adzhigirey, T. Day, R. Annabhimoju, W. Sherman, Protein and ligand preparation: parameters, protocols, and influence on virtual screening enrichments, *J. Comput. Aided Mol. Des.* 27 (2013) 221–234. DOI: 10.1007/s10822-013-9644-8

[27]. S. Genheden, U. Ryde, The MM/PBSA and MM/GBSA methods to estimate ligand-binding affinities, *Expert Opin. Drug Discov.* 10 (2015) 449–461. DOI: 10.1517/17460441.2015.1032936

[28]. P. Lagarias, K. Barkan, E. Tzortzini, et al., Insights to the binding of a selective adenosine A3 receptor antagonist using molecular dynamic simulations, MM-PBSA and MM-GBSA free energy calculations, and mutagenesis, *J. Chem. Inf. Model.* 59 (2019) 5183–5197. DOI: 10.1021/acs.jcim.9b00751

[29]. M.I. Choudhary, M. Shaikh, A. Wahab, A. Rahman, In silico identification of potential inhibitors of key SARS-CoV-2 3CL hydrolase (Mpro) via molecular docking, MMGBSA predictive binding energy calculations, and molecular dynamics simulation. *Plos one*. 15 (2020) e0235030. DOI: 10.1371/journal.pone.0235030

[30]. L. Xie, Z. Deng, J. Zhang,et al., Comparison of flavonoid O-glycoside, C-glycoside and their aglycones on antioxidant capacity and metabolism during in vitro digestion and in vivo, *Foods* 11 (2022) 882. DOI: 10.3390/ foods11060882

[31]. G. Macip, P. Garcia-Segura, J. Mestres-Truyol, et al., Haste makes waste: a critical review of docking-based virtual screening in drug repurposing for SARS-CoV-2 main protease (M-pro) inhibition, *Med. Res. Rev.* 42 (2022) 744–769. DOI: 10.1002/med.21862

[32]. T. Pantsar, A. Poso, Binding affinity via docking: fact and fiction, *Molecules* 23 (2018) 1899. DOI: 10.3390/molecules23081899

[33]. M. Feher, C.I. Williams, Effect of input differences on the results of docking calculations, *J. Chem. Inf. Model.* 49 (2009) 1704–1714. DOI: 10.1021/ci9000629

[34]. G.L. Warren, C.W. Andrews, A.M. Capelli, et al., A critical assessment of docking programs and scoring functions, *J. Med. Chem*. 49 (2006) 5912–5931. DOI: 10.1021/jm050362n

[35]. D. Ramírez, J. Caballero, 2018. Is it reliable to take the molecular docking top scoring position as the best solution without considering available structural data? *Molecules* 23 (2018) 1035. DOI: 10.3390/molecules23051038

[36]. A. Gimeno, M.J. Ojeda-Montes, S. Tomás-Hernández, et al., The light and dark sides of virtual screening: what is there to know? *Int. J. Mol. Sci.* 20 (2019) 1375. DOI: 10.3390/ijms20061375

[37]. L. Pinzi, G. Rastelli, Molecular docking: shifting paradigms in drug discovery, *Int. J. Mol. Sci.* 20 (2019) 4331. DOI: 10.3390/ijms20184331

[38]. S. Megantara, A. Rusdin, A. Budiman, et al., Proving the absence of correlation between molecular docking predictions and in vitro cytotoxicity study in anti-breast cancer drugs development. Preprints. (2024). DOI: 10.20944/preprints202412.0797.v1